European Review for Medical and Pharmacological Sciences 2020; 24: 5703-5713

Natural killer cell-derived exosome-entrapped paclitaxel can enhance its anti-tumor effect

D. HAN[1], K. WANG[1], T. ZHANG[2], G.-C. GAO[1], H. XU[1]

[1]Jiaxing University, Jiaxing, Zhejiang, China
[2]Zhejiang Chinese Medical University, Hangzhou, Zhejiang, China

Abstract. – OBJECTIVE: To study the effectiveness of natural killer cell-derived exosome (NK-Exos)-entrapped paclitaxel (PTX-NK-Exos) in enhancing its anti-tumor effect.

MATERIALS AND METHODS: The NK-Exos were isolated through ultra-high-speed centrifugation, and the PTX-NK-Exos system was constructed via electroporation. The morphology, particle size, Zeta potential and entrapment rate of PTX-NK-Exos were evaluated using transmission electron microscope (TEM), dynamic light scattering (DLS), Western blotting and high-performance liquid chromatography (HPLC), respectively. The uptake of Exos in human breast cancer MCF-7 cells was observed under a laser confocal microscope. Moreover, the effect of PTX-NK-Exos on MCF-7 cell viability was determined through methyl thiazolyl tetrazolium (MTT) assay, flow cytometry and 4',6-diamidino-2-phenylindole (DAPI) staining. The effects of PTX-NK-Exos on messenger ribonucleic acid (mRNA) and protein expressions of B-cell lymphoma-2 (Bcl-2), Bcl-2 associated X protein (Bax) and Caspase-3 in MCF-7 cells were detected using quantitative reverse transcription-polymerase chain reaction (qRT-PCR) and Western blotting, respectively.

RESULTS: The NK-Exos were successfully isolated via ultra-high-speed centrifugation, and they had uniform particle size and high expression of markers for Exos. MCF-7 cells could take up Exos. The PTX-NK-Exos drug delivery system was successfully prepared using electroporation. In PTX group and NK-Exos group, the proliferation of MCF-7 cells declined, the nuclear apoptosis was evident and the apoptosis rate of MCF-7 cells rose compared with those in Control group. In PTX group and PTX-NK-Exos group, the migration of MCF-7 cells declined compared with that in Control group. According to the results of qRT-PCR and Western blotting, PTX-NK-Exos exerted an anti-tumor effect through inducing the up-regulation of Bax and Caspase-3 in the apoptotic signaling pathway in tumor cells.

CONCLUSIONS: Exos isolated through ultra-high-speed centrifugation can be used to prepare the PTX-NK-Exos drug delivery system through electroporation. Drug-loaded Exos can effectively inhibit proliferation and induce apoptosis of tumor cells, thereby exerting an anti-tumor effect.

Key Words:
Exosomes, MCF-7 cells, Apoptosis.

Introduction

Breast cancer is a major disease in females around the world, with such biological characteristics as strong invasiveness, and proneness to recurrence and metastasis. Currently, chemotherapy is still one of the most common therapeutic methods for various tumors. Paclitaxel (PTX), an important chemotherapy drug for tumor, is a kind of basic drug for the clinical treatment of advanced and early ovarian cancer, breast cancer, lung cancer, etc.[1], but its wide clinical application is limited due to its poor water solubility. Although the mixture of castor oil and ethanol (1:1) can dissolve paclitaxel, the dose-dependent toxicity caused by such solvent cannot be ignored. In particular, the biological and pharmacological properties of castor oil can lead to allergic reaction, hyperlipidemia, abnormal lipoprotein pattern, erythrocyte aggregation, and long-term irreversible neurogenic disease[2].

To solve the above problems, Abraxane®, a castor oil-free albumin-bound PTX nano preparation, was approved for marketing by the US Food and Drug Administration in 2005, which displays good pharmacokinetics[3] and therapeutic effects[4]. In phase III clinical trial for women with metastatic breast cancer, Abraxane® has a better therapeutic effect than castor oil-based PTX, but there are still significant declines in leukocytes and erythrocytes and allergic reaction when it is

Corresponding Author: Huang Xu, BM; e-mail: kjrtdsz@163.com

administered via intravenous injection[5]. Therefore, the new drug-loading system is essential for expanding the clinical application of PTX.

Currently, the most commonly used drug carriers are mostly synthesized artificially, such as polymeric drug carriers, causing problems with biocompatibility. Exosomes (Exos) are derived from cells or organisms themselves, and their biocompatibility is undoubtedly excellent compared with other artificially synthesized carriers. Moreover, the related proteins on the surface of Exos are beneficial to the cell phagocytosis, so Exos, as drug carriers, have aroused increasingly more attention and research. Sun et al[6] entrapped the hydrophobic drug curcumin using Exos to improve its solubility and bioavailability, and transnasally delivered the drug to the brain for the treatment of cerebral inflammation. Alvarez-Erviti et al[7] entrapped small-interfering ribonucleic acid (siRNA) into Exos via electroporation and delivered siRNA to the brain after surface targeted modification. In addition, Agrawal et al[8] proved that the milk-derived Exos can entrap PTX and compared with free PTX (30%) at the same dose, the Exos-entrapped system has a high tumor inhibition rate of 60% and mild toxic side effects.

Most importantly, Exos will specifically carry the RNA, protein and other components in parent cells during secretion, and reach the specific sites through body fluid transport to be involved in the *in vivo* signal transduction, tumor immune escape and treatment of related diseases[9,10]. Therefore, the source and physiological state of parent cells determine that the contents carried by Exos are different, and their functions are closely related to the parent cells. It is reported in the literature that natural killer cell-derived Exos (NK-Exos) can inhibit the abnormal proliferation of melanoma cells and raise the survival rate of melanoma mice. Based on this, with NK-Exos as the carrier of PTX, PTX was entrapped into NK-Exos using electroporation in this experiment. It was found that NK-Exos-entrapped PTX (PTX-NK-Exos) significantly inhibited the proliferation of breast cancer cells and had a better therapeutic effect.

Materials and Methods

Reagents

Human NK-92 cells and human breast cancer MCF-7 cells were purchased from Shanghai Cell Bank, Chinese Academy of Sciences, fetal bovine serum (FBS), minimum essential medium-α (MEMα), high-glucose Dulbecco's Modified Eagle's Medium (DMEM) and double antibodies from Gibco (Rockville, MD, USA), TRIzol from Invitrogen (Carlsbad, CA, USA), CD63, Alix and TSG101 antibodies from Abcam, mRNA extraction kit and SYBR Green assay kit from Shanghai BAT Biotechnology Co., Ltd.(Shanghai, China), chloroform, glycerol, methanol, isopropanol and glacial acetic acid (analytically pure) from Sinopharm Chemical Reagent Co., Ltd. (Beijing, China), Tecnai G2 Spirit Biotwin transmission electron microscope (TEM) from Thermo Fisher Scientific (Waltham, MA, USA), Beckman L-90K ultra-high speed refrigerated centrifuge produced by Beckman (Miami, FL, USA), and Malvern Zetasizer Nano ZS90.

Cell Culture

Preparation of endogenous Exos-free FBS[11-13]: FBS was taken and centrifuged at 120,000 g for 16 h, and 5% precipitate at the bottom of tube was discarded to obtain Exos-free FBS. After sterilization using 0.45 μm filter, Exos-free FBS was stored at -80°C for later use.

NK-92 cells were cultured in the MEMα containing 10% Exos-free FBS, and MCF-7 cells were cultured in the DMEM containing 10% FBS and 1% double antibodies. They were all routinely cultured in the constant temperature and humidity sterile incubator with 5% CO_2 at 37°C, and the medium was replaced regularly, followed by subculture when 85-90% cells were fused.

Extraction of Exos

Exos were extracted through ultra-high-speed differential centrifugation[14,15]: The culture supernatant was collected and centrifuged at 300 g for 10 min, 2,000 g for 10 min and 10,000 g for 30 min to remove cells and cell debris. After filtering through the 0.22 μm filter membrane, the filtrate was centrifuged at 120,000 g for 2 h, and the supernatant was discarded. Then, the precipitate was resuspended with an appropriate amount of Exos-free phosphate-buffered saline (PBS), and centrifuged at 120,000 g for another 2 h to remove the residual protein. After the concentration of Exos was measured with bicinchoninic acid (BCA) method (Beyotime, Shanghai, China), Exos were stored at -80°C for later use.

Drug Entrapment

A total of 0.2 μL of Exos and 50 μg of PTX (Taxol) were mixed evenly with buffer (200 μL

system), electroporated at room temperature under 1000 V for 20 ms and stored at 4°C[16]. Then, the blank-NK-Exos (Control group) and PTX-NK-Exos (Experimental group) were obtained.

Identification of Exos

Observation of morphology of Exos under the TEM: 20 μL of Exos obtained using ultra-high-speed centrifugation, PEG precipitation and kit were taken, added dropwise onto the copper mesh, and sucked dry using the filter paper after 1 min. Then, a drop of 1% uranyl acetate was added and sucked dry using the filter paper after 1 min. After drying under the incandescent lamp, Exos were observed and photographed under the TEM.

Determination of Exos particle size *via* dynamic light scattering (DLS): 0.5 mL of Exos mother liquor was taken, added with 4.5 mL of ultrapure water, and filtered with the 0.22 μm filter membrane. Finally, the particle size was detected using the Malvern Zetasizer Nano ZS90.

Analysis of Exos specific proteins using Western blotting: the separated and purified Exos were added with 5× loading buffer, boiled at 100°C for 5 min and cooled to room temperature. After separation via 12% sodium dodecyl sulphate-polyacrylamide gel electrophoresis (SDS-PAGE), the protein in the gel was transferred onto the polyvinylidene difluoride (PVDF) membranes (Millipore, Billerica, MA, USA), sealed with 5% skim milk powder at room temperature for 1 h, and incubated with rabbit anti-human TSG101 monoclonal antibody (1:1000), rabbit anti-human Alix monoclonal antibody (1:1000) and rabbit anti-human CD63 monoclonal antibody (1:1000) at 4°C overnight. After the membrane was washed with Tris-Buffered Saline with Tween-20 (TBST) (5 min × 3 times), the protein was incubated again with horseradish peroxidase (HRP)-labeled goat anti-rabbit IgG secondary antibody at room temperature for 2 h, and the membrane was washed again with TBST (5 min × 3 times). Finally, the protein was detected using the super enhanced chemiluminescence (ECL; Pierce, Rockford, IL, USA) kit.

Analysis of Exos Uptake Under the Laser Confocal Microscope

Exos were labeled with the PKH67 Green Fluorescent Cell Linker Kit dye. NK-Exos were resuspended in 1 mL of diluent C, and PKH67 dye at a final concentration of 4×10^6 mol/L was freshly prepared. According to the instructions, 1 mL of NK-Exos was added into 1 mL of dye for incubation in the dark at room temperature for 4 min, and the staining was terminated using 2 mL of bovine serum albumin (BSA) (0.5%). The labeled NK-Exos were centrifuged again at 120,000 g for 2 h to remove the residual dye. The precipitate was resuspended with 200 μL of PBS. The above dye-labeled NK-Exos were added into a 24-well plate with slides at an original concentration of 20 μg/mL for incubation for 12 h. After washing with PBS (5 min × 3 times), NK-Exos were incubated with 4% PFA for 10 min in the dark, and the fixative was aspirated. After washing with PBS (5 min × 3 times), 500 μL of 4',6-diamidino-2-phenylindole (DAPI) was added into each well for nuclear staining for 10 min, and then DAPI dye was aspirated. After washing with PBS (5 min × 3 times), 100 μL of F-actin (cytoskeleton staining) was added into each well for incubation for 10 min in the dark, and then F-actin was aspirated. After washing with PBS (5 min × 3 times), the slides were sealed with anti-fluorescence quenching buffer. The images of all slides prepared were acquired under the confocal microscope and analyzed using ImageJ software.

Detection of Effect of PTX on Proliferation of MCF-7 Cells Using MTT Assay

4×10^4 MCF-7 cells were inoculated into a 96-well plate. After adherence to the wall, the cells were added with blank NK-Exos (40 μg/mL), Taxol solution (The dose of PTX was 15 μg/mL), PTX-NK-Exos (PTX concentration: 15 μg/mL) and blank control (Control) without any treatment, respectively, with 6 replicates in each group. The culture plate was incubated in the incubator with 5% CO_2 at 37°C for 24, 48, and 72 h, and then, 20 μL of MTT solution was added into each well and placed in the incubator for 4 h. After the supernatant was discarded, 150 μL of DMSO solution was added into each well, and the optical density (OD) value was measured at 490 nm using a microplate reader.

Detection of Apoptosis of MCF-7 Cells Via DAPI Staining

5×10^5 MCF-7 cells were inoculated into a 6-well plate. After adherence to the wall, the cells were added with blank NK-Exos (40 μg/mL), Taxol solution (The dose of PTX was 15 μg/mL), PTX-NK-Exos (PTX concentration: 15 μg/mL) and blank control (Control) without any treatment, respectively, with 3 replicates in each group.

Determination of Apoptosis Rate Through Annexin V-FITC/PI Double Staining

5×10^5 MCF-7 cells were inoculated into the 6-well plate. After adherence to the wall, the cells were added with blank NK-Exos (40 μg/mL), Taxol solution (The dose of PTX was 15 μg/mL), PTX-NK-Exos (PTX concentration: 15 μg/mL) and blank control (Control) without any treatment, respectively, with 3 replicates in each group. After culture for 24 h, the cells were digested with EDTA-free trypsin, centrifuged at 1,000 rpm for 8 min, resuspended with 400 μL of Annexin V binding buffer, and transferred into the 1.5 mL EP tube (Eppendorf, Hamburg, Germany). Then 5 μL of Annexin-FITC staining solution was added and mixed evenly for incubation for 15 min in the dark. Finally, 10 μL of propidium iodide (PI) staining solution was added for incubation for 5 min in the dark, followed by detection using the flow cytometer.

Detection of Cell Migration Ability Via Wound Healing Assay

The culture plate without inoculated cells was marked. After digestion, the cells were inoculated into the 24-well plate, and added with blank NK-Exos (40 μg/mL), Taxol solution (The dose of PTX was 15 μg/mL), PTX-NK-Exos (PTX concentration: 15 μg/mL) and blank control (Control) without any treatment, respectively, for 28 h of treatment, while PBS was added in Control group, with 3 replicates in each group. After the cells fully covered the bottom of plate, they were scratched using a 1 mL pipette tip perpendicular to the plate (try to ensure the same width of each scratch). Then, the cell culture solution was aspirated, and the plate was washed with PBS for 3 times to wash off the cell debris and photographed (T0). After culture for another 24 h, the cell migration was observed and photographed again (T24). Finally, the cell scratch length was measured using ImageJ software, and the cell migration rate was calculated: cell migration rate (%) = (T0 width - T24 width)/T0 width × 100%. The experiment was repeated for 3 times.

Detection of Expressions of B-cell Lymphoma-2 (Bcl-2), Bcl-2 Associated X Protein (Bax) and Caspase-3 Using Quantitative Reverse Transcription-Polymerase Chain Reaction (qRT-PCR)

Cells in each group were lysed with TRIzol lysis buffer, and the total RNA was extracted and synthesized into cDNA according to the instructions. Then, qRT-PCR was performed under the following reaction system: 5 μL of SYBR Taq enzyme, 1 μL of forward primers and 1 μL of reverse primers of Bax, Bcl-2 and Caspase-3, 1 μL of cDNA template, and RNase-free water added until the constant volume of 25 μL, for a total of 40 cycles. The qRT-PCR results were analyzed using $2^{-\Delta\Delta Ct}$ method. Primer sequences used were shown below: Bax-F: 5'-CATGGGCTGGACATTGGACT-3'; Bax-R: 5'-AAAGTAGGAGAGGAGGCCGT-3'. Bcl-2-F: 5'-CTTTGAGTTCGGTGGGGTCA-3'; Bcl-2-R: 5'-GAAATCAAACAGAGGCCGCA-3'. Caspase-3-F: 5'-GGCGCTCTGGTTTTCGTTAATA-3'; Caspase-3-R: 5'-GCTGCATCGACATCTGTACC-3'. GAPDH-F: 5'-CGACCACTTTGTCAAGCTCA-3'; GAPDH-R: 5'-ACTGAGTGTGGCAGGGACTC-3'.

Detection of Protein Expression Levels of Bax, Bcl-2, and Caspase-3 in MCF-7 Cells Through Western Blotting

Cells were washed with PBS and lysed with radioimmunoprecipitation assay (RIPA; Beyotime, Shanghai, China) lysis buffer to extract the total protein in each group. 30 μg of proteins in each group were loaded, subjected to 12% SDS-PAGE, transferred onto the membrane, sealed with 5% skim milk powder solution for 1 h and incubated with Bax, Bcl-2 and Caspase-3 primary antibodies at 4°C overnight. On the next day, the membrane was washed with TBST (5 min × 3 times), and ECL reagent (mixture of solution A and solution B at 1:1) was added for exposure. Finally, the gray value of each band was analyzed using ImageJ software.

Statistical Analysis

All experiments were repeated for at least 3 times, and SPSS 17.0 (SPSS Inc., Chicago, IL, USA) software was used for data processing. Measurement data were expressed as mean ± standard deviation. Comparison between multiple groups was done using One-way ANOVA test followed by post-hoc test (Least Significant Difference). $p<0.05$ suggested that the difference was statistically significant.

Results

Identification of Exos

Results of TEM revealed that the particle size of Exos obtained via ultra-high-speed centrif-

ugation was about 100 nm (Figure 1A, 1B), consistent with that (30-150 nm) reported in the literature. It could be observed via staining that Exos had intact capsule structure in a typical cup shape. In addition, drug-loaded Exos had no significant changes in the morphology (Figure 1B), and they had evident saucer-like double-layer membrane structure, with single distribution or aggregation in groups, and the background was clear with less pollutants.

The particle sizes of NK-Exos and PTX-NK-Exos were detected via DLS (Nano ZS90). As shown in Figure 1C, both mean and median particle sizes of NK-Exos were about 100 nm, and they ranged from 80 to 110, confirming that the particle size of Exos was within the definition. After drug loading, the particle size of PTX-NK-Exos was slightly increased (Figure 1D), consistent with the results in the literature. After drug loading, the particle size of NK-Exos rose, partly

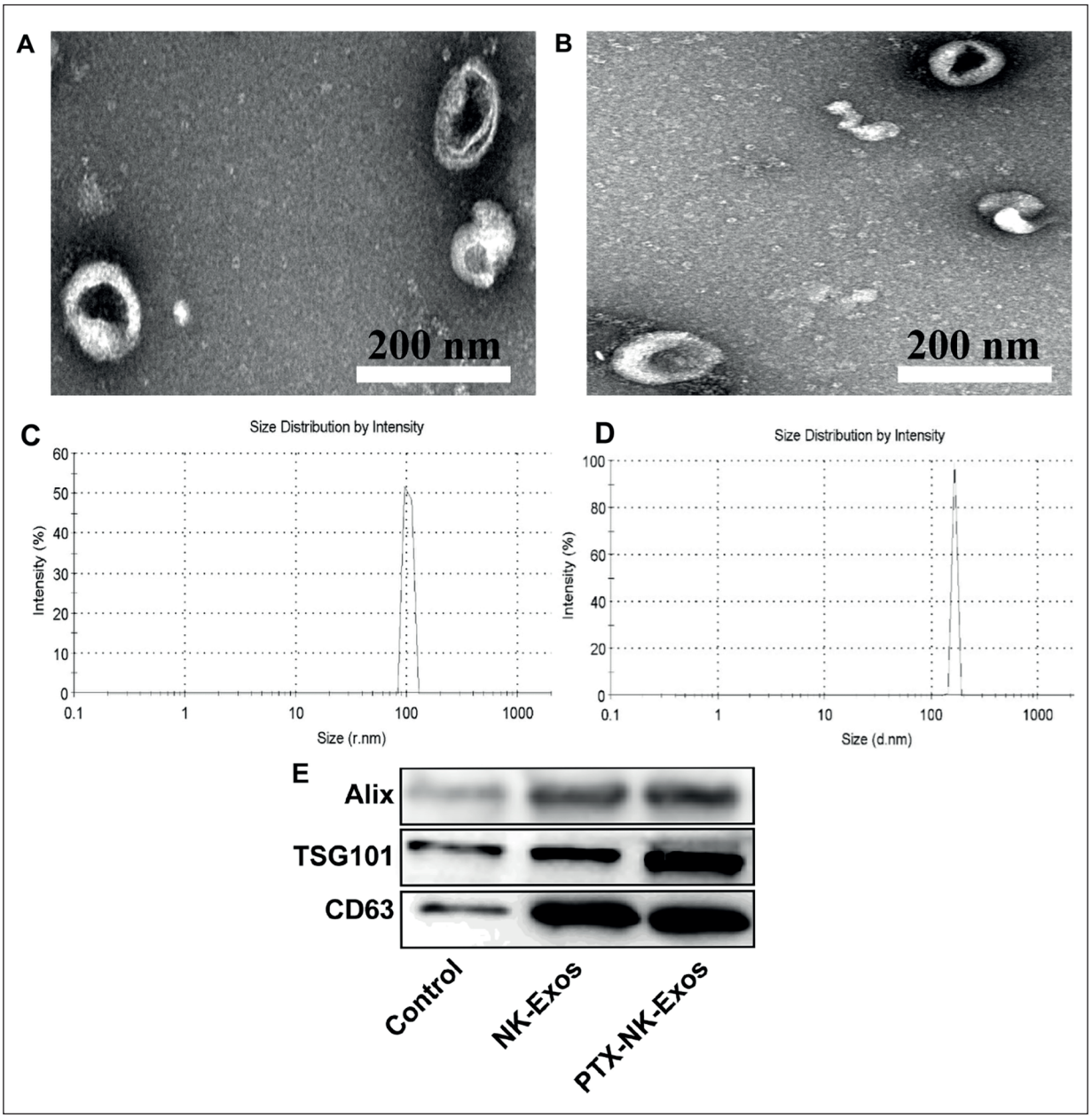

Figure 1. Identification of Exos. **A, B,** Morphology of Exos observed by TEM (magnification: 20, 000 ×). **C, D,** Particle size of NK-Exos analyzed using DLS. **E,** Expressions of Exos specific proteins analyzed using Western blotting.

because of the embedding of PTX into lipid bilayer of Exos and surface adsorption caused by hydrophobic effect[8,17].

The expressions of Exos specific marker proteins were determined using Western blotting, including membrane protein CD63 and inclusion proteins Alix and TSG101 (Figure 1E). It was found that CD6, Alix and TSG101 had positive and significantly higher expressions, suggesting that Exos were obtained via ultra-high-speed centrifugation. There was no evident effect on the expressions of Exos specific proteins after drug loading.

Uptake of Exos

As shown in Figure 2, the blue DAPI indicated the nucleus, the red phalloidine indicated the cytoskeleton, and the green PKH67 indicated the Exos. In the Merge graph, green fluorescence was clearly visible, mainly in the cytoplasm. The 4T1 cytoskeletal protein F-actin stained by phalloidine was labeled with Rhodamine 123, and red fluorescence could also be clearly seen in 4T1, indicating that PKH-67-labeled Exos can be taken in by MCF-7 cells.

PTX-NK-Exos Promoted Apoptosis of MCF-7 Cells

According to the results of MTT assay (Figure 3A-3C), the MCF-7 cell viability significantly declined in PTX group and NK-Exos group compared with that in Control group at 24 h, 48 h and 72 h ($^{*}p<0.05$, $^{*}p<0.05$, $^{*}p<0.05$). The MCF-7 cell viability also significantly declined in PTX-NK-Exos group compared with that in PTX group. ($^{\#\#}p<0.01$, $^{\#\#}p<0.01$, $^{\#\#}p<0.01$). Moreover, the results of DAPI staining and flow cytometry (Figure 3D-3F), consistent with those of MTT assay, showed that the inhibitory effects of PTX and PTX-NK-Exos at the same concentration on proliferation of MCF-7 cells were more significant than that of free PTX ($^{*}p<0.05$), but there was no significant difference in the inhibitory effect on proliferation of MCF-7 cells between NK-Exos and PTX.

Effect of PTX-NK-Exos on Migration Ability of MCF-7 Cells

The results of wound healing assay manifested that the migration rate of MCF-7 cells declined in NK-Exos group and PTX group compared with that in Control group ($^{*}p<0.05$), while it was evidently decreased in PTX-NK-Exos group compared with that in PTX group ($^{\#\#}p<0.01$) (Figure 4).

Effects of PTX-NK-Exos on mRNA Expressions of Bax, Bcl-2, and Caspase-3 in MCF-7 Cells

According to the results of qRT-PCR (Figure 5A, 5B), the mRNA expressions of Bax, Bcl-2 and Caspase-3 in MCF-7 cells remarkably rose in NK-Exos group and PTX group compared with those in Control group ($^{*}p<0.05$), while they were also remarkably up-regulated in PTX-NK-Exos group compared with those in PTX group ($^{\#\#}p<0.01$).

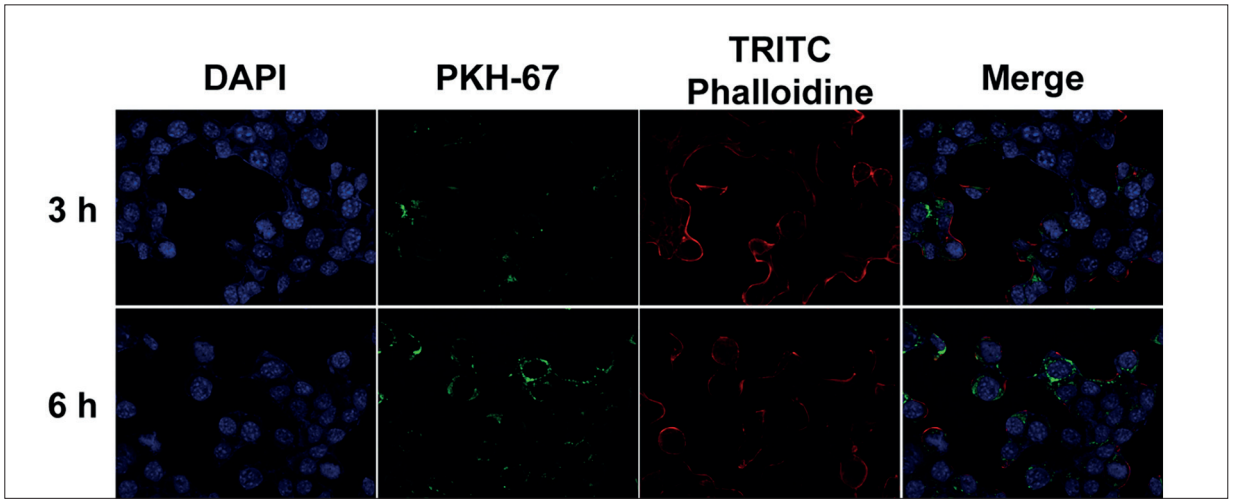

Figure 2. Uptake of Exos. Uptake of Exos in MCF-7 cells is observed using the laser confocal microscope. DAPI-stained nuclei, PKH67-stained Exos, and Rhodamine-labeled phalloidine-stained cytoskeleton (magnification: 400 ×).

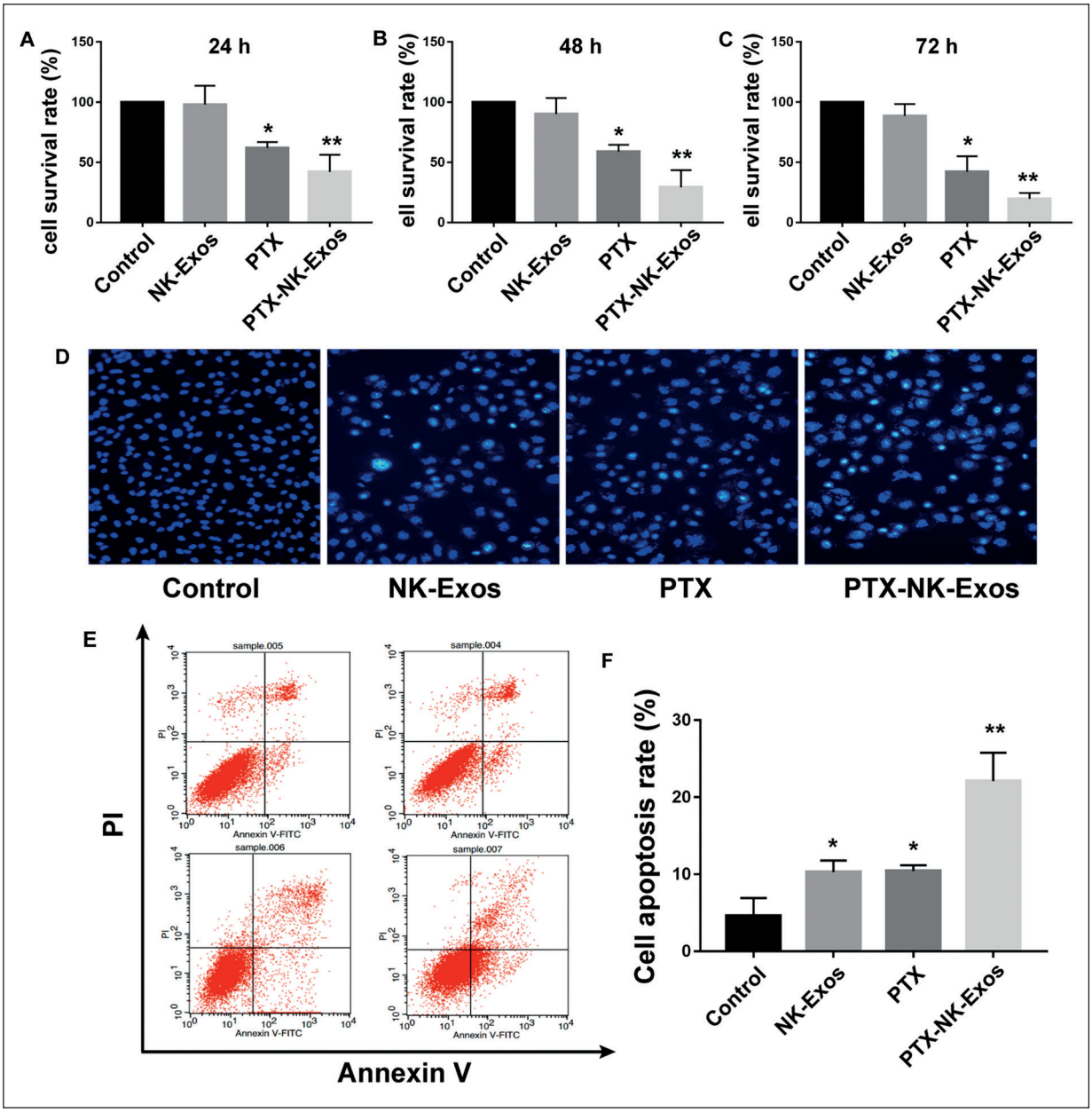

Figure 3. MCF-7 cell apoptosis assay. **A-C,** Survival rate of MCF-7 cells at 24 h, 48 h and 72 h detected using MTT assay. **D,** Apoptosis of MCF-7 cells detected using DAPI staining (magnification: 100 ×). **E, F,** Apoptosis rate of MCF-7 cells after drug administration detected using flow cytometry.

Effects of PTX-NK-Exos on Protein Expressions of Bax, Bcl-2, and Caspase-3 in MCF-7 Cells

According to the results of Western blotting (Figure 5C-5E), the protein expressions of Bax, Bcl-2 and Caspase-3 in MCF-7 cells remarkably rose in NK-Exos group and PTX group compared with those in Control group (*p<0.05), while they were also remarkably up-regulated in PTX-NK-Exos group compared with those in PTX group ($^{\#\#}p$<0.01).

Discussion

PTX is a kind of important anti-tumor drug that plays an important role in the treatment of various malignant tumors, such as breast cancer[8]. However, the dose-dependent toxicity of PTX greatly restricts its widespread application in clinic. In recent years, the naturally sourced nanoscale drug carrier Exos has been used to deliver a variety of chemotherapy drugs to spe-

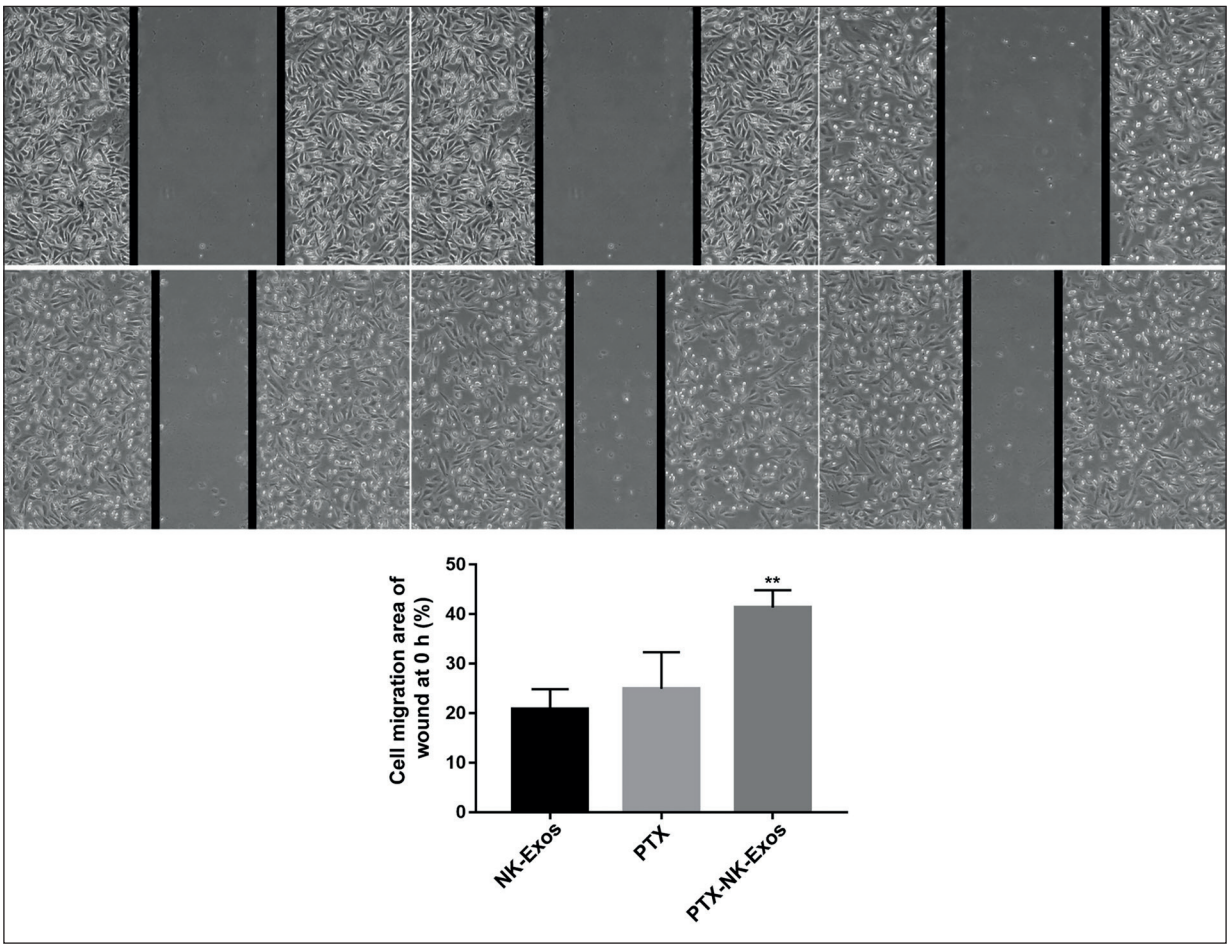

Figure 4. PTX-NK-Exos inhibits migration of MCF-7 cells (magnification: 50 ×).

cific tissues and cells *in vivo*[18], especially tumor tissues[19]. Exos possess the properties of parent cells, and its role in intercellular communication and signal transduction has attracted increasingly more attention[20,21]. Wan et al[17] found that Exos from tumor tissues can regulate the tumor immune response, facilitate the tumor metastasis, and induce the resistance of tumor cells to chemotherapy drugs. Exos isolated from milk has the intrinsic anti-tumor activity[22,23], and NK-Exos has toxic side effects on melanoma cells *in vitro*. Moreover, it was found in the research for tumor mice that Exos can significantly inhibit tumor growth *in vivo*[24]. At the same time, Exos has good compatibility and it is widely explored as a drug carrier, which can simultaneously delivery hydrophobic and hydrophilic cargos. Besides, NK-Exos itself can exert an inhibitory effect on melanoma. Therefore, NK-Exos were used as the delivery system for PTX in this study.

In this investigation, the PTX-NK-Exos delivery system was successfully prepared. The particle size of Exos was first detected via DLS before and after drug loading. It was found that the mean particle size of Exos was increased from 104 nm to 141.6 nm after drug loading. Yuan et al[18] have shown that PTX will be partially embedded in the lipid bilayer of Exos during entrapment, resulting in a slight increase in the particle size of Exos after drug loading. To determine the effect of drug loading on the property of Exos, the surface protein, morphology and potential of Exos were further evaluated. The results of Western blotting manifested that the drug loading process did not affect the protein abundance of Exos. The TEM results showed that after drug loading, the morphology and structure of Exos basically remained unchanged, but its potential slightly declined, consistent with the results obtained by other researchers[18,25]. Therefore, the drug loading process has

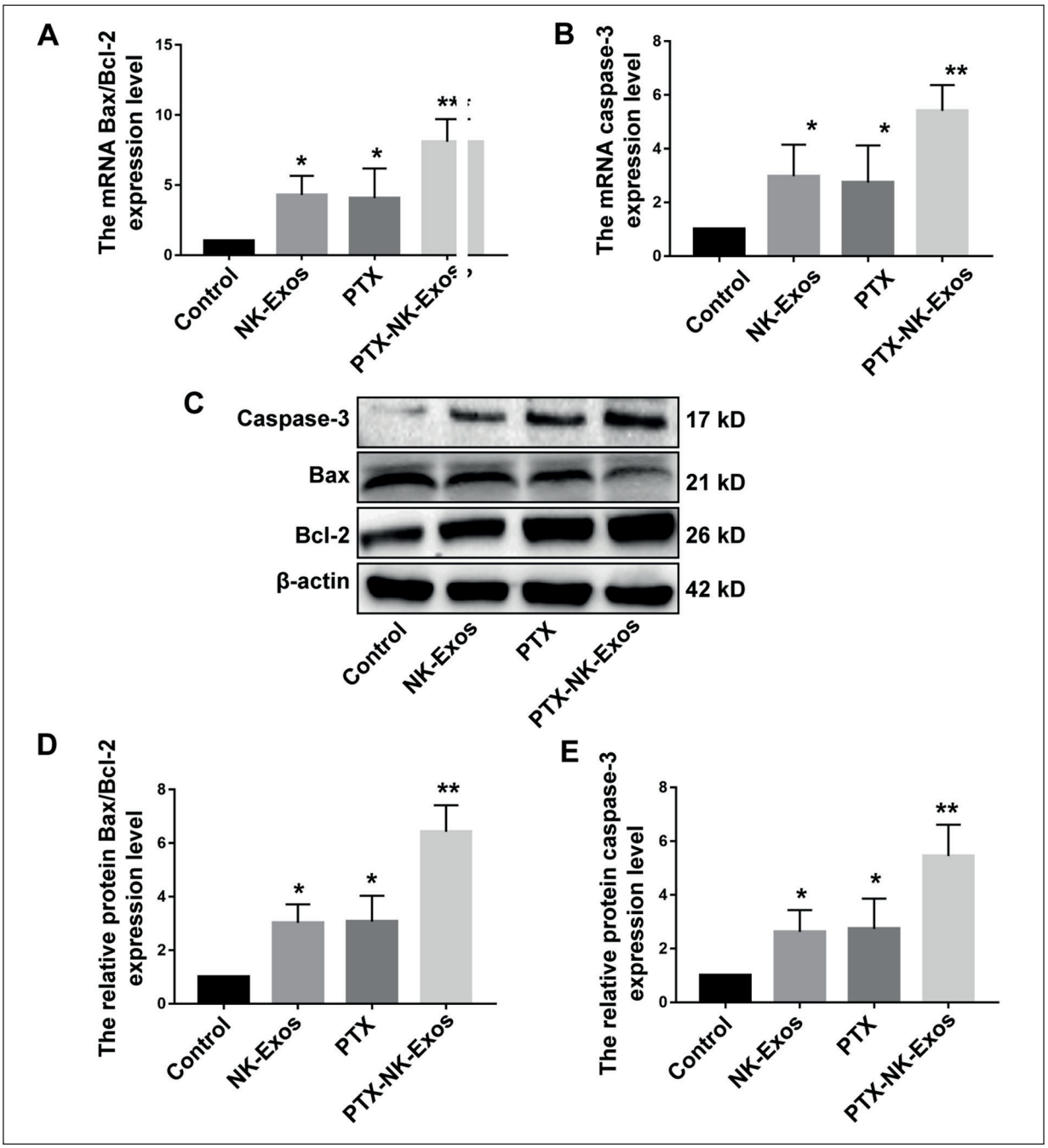

Figure 5. Expressions of apoptosis proteins in MCF-7 cells determined using qRT-PCR and Western blotting. **A, B,** MRNA levels of Bax, Bcl-2 and Caspase-3 in MCF-7 cells detected *via* qRT-PCR. **C-E,** Protein levels of Bax, Bcl-2 and Caspase-3 in MCF-7 cells detected *via* Western blotting.

no significant effects on the morphology and structure of Exos, and all properties of Exos are preserved after drug loading.

According to the anti-tumor experiment, the PTX-NK-Exos drug loading system at the same dose had a higher inhibition rate on human breast cancer MCF-7 cells compared with free PTX. Such a phenomenon has been explained by some studies, and it has been found that the lipid bilayer of Exos can directly target and fuse cells, thereby enhancing cellular internalization of PTX and improving the therapeutic effect. However, there

are some limitations. This procedure cannot be used for all drugs. Electroporation is traditionally considered as means to introduce DNA, RNA, enzymes, drugs or biochemical reagents into cells. Generally, RNAs and other hydrophilic compounds can be loaded into exosomes by electroporation. The principle of this method is to create countless pores on the exosome membrane under short and high-voltage pulses, thus allowing the penetration of drug molecules into the exosomes. Taxol is a kind of important anti-tumor drug that plays an important role in the treatment of breast cancer. However, the dose-dependent toxicity of PTX greatly restricts its widespread application in clinic. NK-exosomes exhibited toxic effects on melanoma cells *in vitro*. Moreover, it has reported that NK-exosomes can significantly inhibit the tumor growth *in vivo*. So, when Taxol was carried by NK-exosomes, low-dose taxol has better anti-tumor effect[7,24-27].

Conclusions

In this paper, with the clinically widely used PTX as a model drug, NK-Exos were extracted from NK cells via classical ultra-high-speed centrifugation and used as the PTX delivery system. The PTX-NK-Exos system was prepared via electroporation, so that the delivery system of chemotherapy drugs carried by natural carrier was constructed successfully. Moreover, the carrier was extracted, the drug delivery system was prepared, and the characterization and *in vitro* pharmacodynamic activity were evaluated, thereby further verifying the anti-tumor activity of drug loading system.

Conflict of Interest

The Authors declare that they have no conflict of interests.

Funding Acknowledgements

Experimental Animal Research Project of Zhejiang Science and Technology Department

References

1) Wang P, Wang H, Huang Q, Peng C, Yao L, Chen H, Qiu Z, Wu Y, Wang L, Chen W. Exosomes from M1-Polarized macrophages enhance paclitaxel antitumor activity by activating macrophages-mediated inflammation. Theranostics 2019; 9: 1714-1727.
2) Gelderblom H, Verweij J, Nooter K, Sparreboom A. Cremophor EL: the drawbacks and advantages of vehicle selection for drug formulation. Eur J Cancer 2001; 37: 1590-1598.
3) Sparreboom A, Scripture CD, Trieu V, Williams PJ, De T, Yang A, Beals B, Figg WD, Hawkins M, Desai N. Comparative preclinical and clinical pharmacokinetics of a cremophor-free, nanoparticle albumin-bound paclitaxel (ABI-007) and paclitaxel formulated in Cremophor (Taxol). Clin Cancer Res 2005; 11: 4136-4143.
4) Gradishar WJ, Tjulandin S, Davidson N, Shaw H, Desai N, Bhar P, Hawkins M, O'Shaughnessy J. Phase III trial of nanoparticle albumin-bound paclitaxel compared with polyethylated castor oil-based paclitaxel in women with breast cancer. J Clin Oncol 2005; 23: 7794-7803.
5) Bawarski WE, Chidlowsky E, Bharali DJ, Mousa SA. Emerging nanopharmaceuticals. Nanomedicine 2008; 4: 273-282.
6) Sun D, Zhuang X, Xiang X, Liu Y, Zhang S, Liu C, Barnes S, Grizzle W, Miller D, Zhang HG. A novel nanoparticle drug delivery system: the anti-inflammatory activity of curcumin is enhanced when encapsulated in exosomes. Mol Ther 2010; 18: 1606-1614.
7) Alvarez-Erviti L, Seow Y, Yin H, Betts C, Lakhal S, Wood MJ. Delivery of siRNA to the mouse brain by systemic injection of targeted exosomes. Nat Biotechnol 2011; 29: 341-345.
8) Agrawal AK, Aqil F, Jeyabalan J, Spencer WA, Beck J, Gachuki BW, Alhakeem SS, Oben K, Munagala R, Bondada S, Gupta RC. Milk-derived exosomes for oral delivery of paclitaxel. Nanomedicine-Uk 2017; 13: 1627-1636.
9) Peinado H, Aleckovic M, Lavotshkin S, Matei I, Costa-Silva B, Moreno-Bueno G, Hergueta-Redondo M, Williams C, Garcia-Santos G, Ghajar C, Nitadori-Hoshino A, Hoffman C, Badal K, Garcia BA, Callahan MK, Yuan J, Martins VR, Skog J, Kaplan RN, Brady MS, Wolchok JD, Chapman PB, Kang Y, Bromberg J, Lyden D. Melanoma exosomes educate bone marrow progenitor cells toward a pro-metastatic phenotype through MET. Nat Med 2012; 18: 883-891.
10) Andreola G, Rivoltini L, Castelli C, Huber V, Perego P, Deho P, Squarcina P, Accornero P, Lozupone F, Lugini L, Stringaro A, Molinari A, Arancia G, Gentile M, Parmiani G, Fais S. Induction of lymphocyte apoptosis by tumor cell secretion of FasL-bearing microvesicles. J Exp Med 2002; 195: 1303-1316.
11) Eitan E, Zhang S, Witwer KW, Mattson MP. Extracellular vesicle-depleted fetal bovine and human sera have reduced capacity to support cell growth. J Extracell Vesicles 2015; 4: 26373.
12) Yu G, Jung H, Kang YY, Mok H. Comparative evaluation of cell- and serum-derived exosomes to

deliver immune stimulators to lymph nodes. Biomaterials 2018; 162: 71-81.

13) Zhang Y, Liu Y, Liu H, Tang WH. Exosomes: biogenesis, biologic function and clinical potential. Cell Biosci 2019; 9: 19.

14) Lunavat TR, Jang SC, Nilsson L, Park HT, Repiska G, Lasser C, Nilsson JA, Gho YS, Lotvall J. RNAi delivery by exosome-mimetic nanovesicles - implications for targeting c-Myc in cancer. Biomaterials 2016; 102: 231-238.

15) Du W, Zhang K, Zhang S, Wang R, Nie Y, Tao H, Han Z, Liang L, Wang D, Liu J, Liu N, Han Z, Kong D, Zhao Q, Li Z. Enhanced proangiogenic potential of mesenchymal stem cell-derived exosomes stimulated by a nitric oxide releasing polymer. Biomaterials 2017; 133: 70-81.

16) Wlaschek M, Tantcheva-Poor I, Naderi L, Ma W, Schneider LA, Razi-Wolf Z, Schuller J, Scharffetter-Kochanek K. Solar UV irradiation and dermal photoaging. J Photochem Photobiol B 2001; 63: 41-51.

17) Wan Y, Wang L, Zhu C, Zheng Q, Wang G, Tong J, Fang Y, Xia Y, Cheng G, He X, Zheng SY. Aptamer-conjugated extracellular nanovesicles for targeted drug delivery. Cancer Res 2018; 78: 798-808.

18) Yuan D, Zhao Y, Banks WA, Bullock KM, Haney M, Batrakova E, Kabanov AV. Macrophage exosomes as natural nanocarriers for protein delivery to inflamed brain. Biomaterials 2017; 142: 1-12.

19) Zhang W, Yu ZL, Wu M, Ren JG, Xia HF, Sa GL, Zhu JY, Pang DW, Zhao YF, Chen G. Magnetic and folate functionalization enables rapid isolation and enhanced tumor-targeting of cell-derived microvesicles. ACS Nano 2017; 11: 277-290.

20) Simons M, Raposo G. Exosomes--vesicular carriers for intercellular communication. Curr Opin Cell Biol 2009; 21: 575-581.

21) Thery C, Ostrowski M, Segura E. Membrane vesicles as conveyors of immune responses. Nat Rev Immunol 2009; 9: 581-593.

22) Munagala R, Aqil F, Jeyabalan J, Agrawal AK, Mudd AM, Kyakulaga AH, Singh IP, Vadhanam MV, Gupta RC. Exosomal formulation of anthocyanidins against multiple cancer types. Cancer Lett 2017; 393: 94-102.

23) Munagala R, Aqil F, Jeyabalan J, Gupta RC. Bovine milk-derived exosomes for drug delivery. Cancer Lett 2016; 371: 48-61.

24) Zhu L, Kalimuthu S, Gangadaran P, Oh JM, Lee HW, Baek SH, Jeong SY, Lee SW, Lee J, Ahn BC. Exosomes derived from natural killer cells exert therapeutic effect in melanoma. Theranostics 2017; 7: 2732-2745.

25) Tian Y, Li S, Song J, Ji T, Zhu M, Anderson GJ, Wei J, Nie G. A doxorubicin delivery platform using engineered natural membrane vesicle exosomes for targeted tumor therapy. Biomaterials 2014; 35: 2383-2390.

26) Weaver JC. Electroporation: a general phenomenon for manipulating cells and tissues. J Cell Biochem 1993; 51: 426-435.

27) Gilligan KE, Dwyer RM. Engineering exosomes for cancer therapy. Int J Mol Sci 2017; 18: 1122.